

Investigating the Influence of Heat Radiation on MHD Viscoelastic Nanofluid Flow over a Stretching Sheet with Heat Source and Slip Conditions: A Numerical Analysis.

K saikumar, Koneru Lakshmaiah Education Foundation, India-522302,

Abstract

This study investigates the heat and mass transfer rates in an MHD viscoelastic nanofluid flow, specifically employing Walter's liquid-B model. The flow occurs over a stretching sheet subjected to heat generation/absorption and thermal radiation. The mathematical framework adheres to the fundamental principles of motion and heat transfer. By employing similarity transformations, the governing equations are transformed into a set of nonlinear ordinary differential equations (ODEs). Utilizing the Homotopy Analysis Method (HAM), we obtain numerical solutions for these nonlinear ODEs and their associated boundary conditions. Graphical analysis is conducted to examine the behavior of the resultant equations under the influence of various flow parameters. It is observed that the heat transfer rate diminishes with an increase in the Brownian motion parameter, while it improves with an increase in the thermophoresis parameter. Higher values of the viscoelastic and stretching parameters lead to accelerated velocity slip. The viscoelastic nature of the nanofluid results in reduced values for local skin friction, Nusselt, and Sherwood numbers. Notably, the slip parameter has a significant impact on flow velocity.

Introduction

Magnetohydrodynamics (MHD) is concerned with the study of electrically conductive fluid flow in the presence of a magnetic field, whether it's externally applied or generated within the fluid due to its motion [1]. These flows find a wide range of applications across diverse fields, from industrial processes like steel casting and nuclear fusion reactor heat exchangers, to areas such as bio plasma, medicine, and nanotechnologies. Electrically conductive fluids are integral to numerous industrial and technological processes, with examples including liquid metals like aluminium, mercury, or crucible steel [2-4]. The interaction between a moving fluid and a magnetic field leads to various MHD phenomena that can be harnessed for various purposes. Technological processes leverage electromagnetic flow control to stabilize melts, create fine powders, produce semiconductors, aluminium, and superalloys with exceptional properties [5]. In the realm of fusion reactors, where plasma is manipulated by intense magnetic fields, the exploration of MHD phenomena has surged. Recent research highlights the potential of electromagnetohydrodynamic (EMHD) flows for efficiently transporting low-conductivity fluids within microsystems. These microfluidic devices facilitate the transportation of multiple fluids, enabling tasks like increasing the velocity of one fluid through interaction with a more mobile fluid, enhancing heat transfer, or achieving controlled fluid mixing. The origins of magneto hydrodynamics are often attributed to Hartmann and

Lazarus [6], who conducted pioneering experiments with liquid metals in 1937. Julius Hartmann delved into various technical processes, attempting to create an electromagnetic conduction pump for transporting conductive fluids [7]. Following their work, a few researchers studied scenarios such as Couette flow of conductive viscous fluid between parallel plates in the presence of a perpendicular magnetic field [8]. These studies revealed that a magnetic field and resulting induced currents significantly alter velocity profiles, giving rise to high-velocity gradient boundary layers near the plates. The diverse range of electrically conductive fluids opens up extensive possibilities for the application and advancement of magnetohydrodynamics [9]. One noteworthy category of such fluids, which garnered attention in the latter half of the twentieth century, is nanofluids.

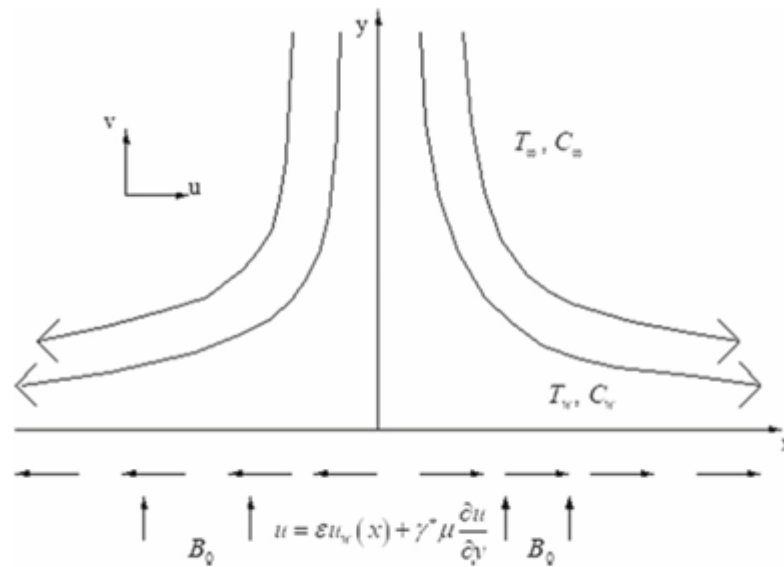


Fig. 1 The system's physical model

Mathematical formulation

Take into consideration the flow of a viscoelastic nanofluid in a boundary layer that is steady over a stretching sheet. While the y-axis denoted by y is measured normal to the sheet, the x-axis denoted by x is taken along its sheet.

$$\frac{\partial u}{\partial x} + \frac{\partial v}{\partial y} = 0, \quad (1)$$

$$u \frac{\partial u}{\partial x} + v \frac{\partial u}{\partial y} = v \frac{\partial^2 u}{\partial y^2} - \frac{k_0}{\rho} \left(u \frac{\partial^3 u}{\partial x \partial y^2} + u \frac{\partial u}{\partial x} \frac{\partial^2 u}{\partial y^2} + \frac{\partial u}{\partial y} \frac{\partial^2 v}{\partial y^2} + v \frac{\partial^3 u}{\partial y^3} \right) - \frac{\sigma B_0(x)^2}{\rho} u, \quad (2)$$

$$u \frac{\partial T}{\partial x} + v \frac{\partial T}{\partial y} = \alpha \frac{\partial^2 T}{\partial y^2} + \tau \left[D_B \frac{\partial c}{\partial y} \frac{\partial T}{\partial y} + \frac{D_T}{D_\infty} \left(\frac{\partial T}{\partial y} \right)^2 \right] - \frac{1}{(\rho c_p)} \frac{\partial q_r}{\partial y} + \frac{Q_0}{(\rho c_p)} (T - T_\infty), \quad (3)$$

$$u \frac{\partial C}{\partial x} + v \frac{\partial C}{\partial y} = D_B \frac{\partial^2 C}{\partial y^2} + \frac{D_T}{D_\infty} \frac{\partial^2 T}{\partial y^2}, \quad (4)$$

The corresponding boundary conditions are given by,

$$u = \varepsilon u_w(x) + \gamma^* \mu \frac{\partial u}{\partial y}, v = 0, T = T_w, C = C_w \text{ at } y = 0 \quad (5)$$

$$u = 0, T \rightarrow T_\infty, C \rightarrow C_\infty \text{ as } y \rightarrow \infty,$$

Methodology

$$(1 - p) L_1(f(\zeta; p) - f_0(\zeta)) = p \hbar_1 N_1[f(\zeta; p)],$$

$$(1 - p) L_2(\theta(\zeta; p) - \theta_0(\zeta)) = p \hbar_2 N_2[f(\zeta; p), \theta(\zeta; p), \varphi(\zeta; p)],$$

$$(1 - p) L_3(\varphi(\zeta; p) - \varphi_0(\zeta)) = p \hbar_3 N_3[f(\zeta; p), \theta(\zeta; p), \varphi(\zeta; p)],$$

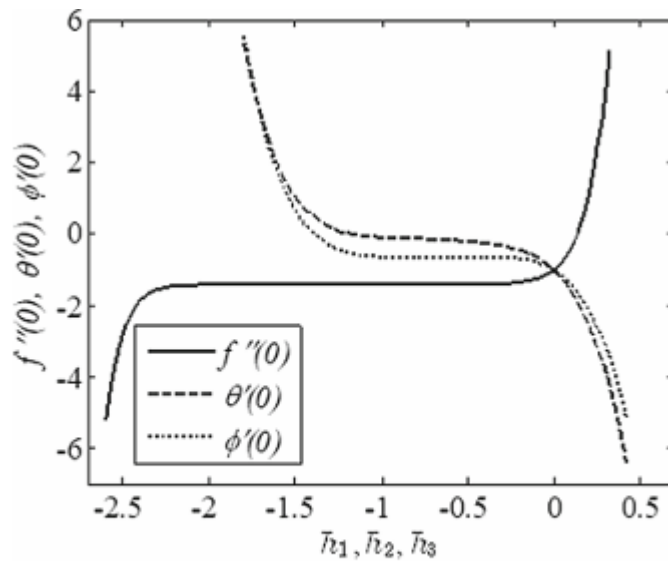


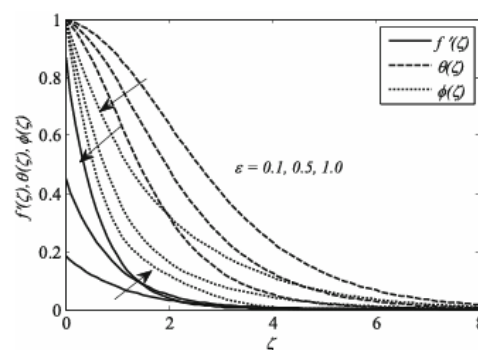
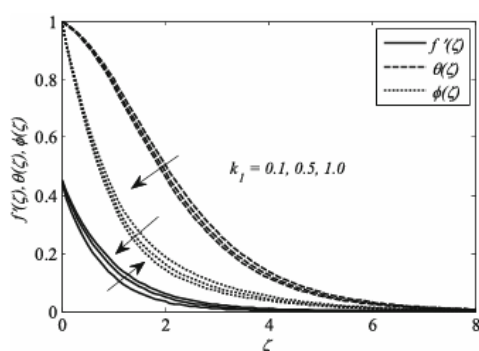
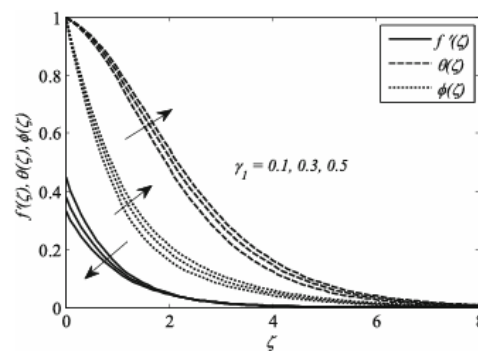
Fig.2 h -curves of $f''(0)$, $\theta'(0)$ and $\phi'(0)$

Results

This section makes use of the supplementary diagrams to investigate how the parameters of the current issue establish the momentum, temperature, and concentration of the viscoelastic nanofluid. Some of the figures are produced by adjusting a parameter within a set range, while others are held constant [10-11].

Table 1 HAM solutions converge for various orders of approximation

Order	$-f''(0)$	$-\theta'(0)$	$-\phi'(0)$
5	0.498384	0.158699	0.781779
10	0.498458	0.155700	0.788359
15	0.498459	0.155339	0.787803
20	0.498459	0.155295	0.787858
25	0.498459	0.155288	0.787853
30	0.498459	0.155287	0.787852
35	0.498459	0.155286	0.787852
40	0.498459	0.155286	0.787852
45	0.498459	0.155286	0.787852

**Fig. 4** Impact of ε on $f'(\zeta)$, $\theta(\zeta)$ and $\phi(\zeta)$ **Fig. 3** Impact of k_1 on $f'(\zeta)$, $\theta(\zeta)$ and $\phi(\zeta)$ **Fig. 5** Impact of γ_1 on $f'(\zeta)$, $\theta(\zeta)$ and $\phi(\zeta)$

Conclusion

We investigate the impact of a uniform magnetic field on the flow and heat transfer characteristics of a non-Newtonian nanofluid over a stretching sheet featuring both a heat source and a heat sink. This analysis also encompasses the influence of thermophoresis and Brownian motion. Employing the Homotopy Analysis Method (HAM), we scrutinize velocity, temperature, and concentration distributions, as well as skin friction, local Nusselt numbers, and local Sherwood numbers across a broad spectrum of control parameters. The findings lead to the following conclusions:

- Increasing the viscoelastic parameter leads to an augmentation in both the momentum boundary layer thickness and velocity, while concentrations and temperature decrease.
- Enhanced slip of the fluid along the stretching surface corresponds to a reduction in the velocity distribution of the flow.
- Elevated heat source or heat sink parameters correlate with increased temperatures. As fluid temperature rises, viscosity decreases, resulting in a thinner thermal boundary layer.
- The viscoelastic nature of the nanofluid contributes to a decrease in local skin friction, local Nusselt number, and local Sherwood number.

References

1. Hartmann, J., Hg-Dynamics, I.: Theory of the laminar flow of an electrically conductive liquid in a homogenous magnetic field. DetKgl Danske Videnskabernes Selskab-Fysiske Meddelelser, XV 6, 1–22 (1937)
2. Lehnert, B.: On the behaviour of an electrically conductive liquid in a magnetic field. Arkiv Fysik 5, 69–90 (1952)
3. U.S.Choi, Enhancing thermal conductivity of fluids with nanoparticles, The Proceedings of the 1995 ASME International Mechanical Engineering Congress and Exposition, San Francisco, CA, ASME, FED231/MD 66, 99–105, 1995.
4. Abu-Nada, E., Oztop, H.F.: Effects of inclination angle on natural Convection in enclosures filled with Cu-water nanofluid. Int. J. Heat Fluid Flow 30, 669–678 (2009)
5. Zargartalebi, H., Ghalambaz, M., Noghrehabadi, A., Chamkha, A.J.: Stagnation point heat transfer of nanofluids toward stretching sheets with variable thermo-physical properties. Adv. Power Technol. 26, 819–829 (2015)
6. Makinde, O.D., Aziz, A.: Boundary layer flow of a nanofluid past a stretching sheet with a convective boundary condition. Int. J. Thermal Sci. 50(7), 1326–1332 (2011)
7. Ibrahim, S.M., Lorenzini, G., Vijayakumar, P., Raju, C.S.K.: Influence of chemical reaction and heat source on dissipative MHD mixed convection flow of a Casson nanofluid over a nonlinear permeable stretching sheet. Int. J. Heat and Mass Transfer 111, 346–355 (2017)
8. Ibrahim, S.M., Kumar, P.V., Lorenzini, G.: Analytical modelling of heat and mass transfer of radiative MHD Casson fluid over an exponentially permeable stretching sheet with chemical reaction. J. Eng. Thermophys. 29(1), 136–155 (2020)
9. Hayat, T., Khan, W.A., Abbas, S.Z.: Impact of induced magnetic field on second-grade nanofluid flow past a convectively heated stretching sheet. Appl. Nanosci. 10, 3001–3009 (2020)
10. Mabod, F.M., Ibrahim, S.M., Kumar, P.V., Lorenzini, G.: Effects of slip and radiation on convective MHD Casson nanofluid flow over a stretching sheet influenced by variable viscosity. J. Eng. Thermophys. 29, 303–315 (2020)
11. Sheremet, M.A., Dinarvand, S., Pop, I.: Effect of thermal stratification on free convection in a square porous cavity filled with nanofluid using Tiwari and Das' nanofluid model. Physica E 69,332–341 (2015)
12. Raju, K., Pilli, S. K., Kumar, G. S. S., Saikumar, K., & Jagan, B. O. L. (2019). Implementation of natural random forest machine learning methods on multi spectral image compression. Journal of Critical Reviews, 6(5), 265-273.
13. Saba, S. S., Sreelakshmi, D., Kumar, P. S., Kumar, K. S., & Saba, S. R. (2020). Logistic regression machine learning algorithm on MRI brain image for fast and accurate diagnosis. International Journal of Scientific and Technology Research, 9(3), 7076-7081.